Ahuva Cern, Ayelet Michael-Gayego, Yaelle Bavli, Erez Koren[a], Amiram Goldblum, Allon E. Moses, Yan Q. Xiong and Yechezkel Barenholz*

Nano-mupirocin: enabling the parenteral activity of mupirocin

DOI 10.1515/ejnm-2016-0006
Received March 16, 2016; accepted April 27, 2016; previously published online June 3, 2016

Abstract: Mupirocin is an antibiotic having a unique mode of action, not shared by any other therapeutically available antibiotic. However, due to its rapid elimination following injection and high protein binding, current therapeutic use is limited to topical administration. Computational methods have identified mupirocin as a good candidate for delivery via long-circulating nano-liposomes. Formulating mupirocin in such liposomes to form Nano-mupirocin protects the drug in the circulation, enabling therapeutic efficacy. This was demonstrated using two different animal models that served as a proof of concept: the mice *necrotizing fasciitis* and rabbit *endocarditis* models. In both animal models, mupirocin administered intravenously (IV) lacked therapeutic efficacy, while the Nano-mupirocin administered IV was efficacious. In both mice and rabbits the pharmacokinetic (PK) profile following IV injection of Nano-mupirocin showed significantly greater AUC and elimination half-life of Nano-mupirocin compared to the free drug. In addition, in mice we also demonstrated significant drug distribution into the disease site. These PK profiles may explain Nano-mupirocin's superior therapeutic efficacy. To the best of our knowledge, this is the first study demonstrating that systemic activity of mupirocin is feasible. Therefore, Nano-mupirocin can be considered a novel and unique parenteral antibiotic candidate drug.

Keywords: antibiotic; computer-based identification; nano-liposomes; repurposing.

[a]**Present address:** Teva Pharmaceutical Industries, Ltd., Kfar Saba, Israel.
***Corresponding author: Yechezkel Barenholz,** Laboratory of Membrane and Liposome Research, Department of Biochemistry, IMRIC, The Hebrew University – Hadassah Medical School, Jerusalem, Israel, Phone: +972 2 6757615, Fax: +972 2 6757499, E-mail: chezyb@ekmd.huji.ac.il
Ahuva Cern: Laboratory of Membrane and Liposome Research, Department of Biochemistry, IMRIC, The Hebrew University – Hadassah Medical School, Jerusalem, Israel; and Molecular Modeling and Drug Design Laboratory, The Institute for Drug Research, The Hebrew University of Jerusalem, Israel
Ayelet Michael-Gayego: Microbial Molecular Diagnostics Laboratory, Department of Clinical Microbiology and Infectious Diseases, Hadassah Hebrew University Medical Center, Jerusalem, Israel
Yaelle Bavli: Laboratory of Membrane and Liposome Research, Department of Biochemistry, IMRIC, The Hebrew University – Hadassah Medical School, Jerusalem, Israel
Erez Koren: Laboratory of Membrane and Liposome Research, Department of Biochemistry, IMRIC, The Hebrew University – Hadassah Medical School, Jerusalem, Israel
Amiram Goldblum: Molecular Modeling and Drug Design Laboratory, The Institute for Drug Research, The Hebrew University of Jerusalem, Israel
Allon E. Moses: Department of Clinical Microbiology and Infectious Diseases, Hadassah Hebrew University Medical Center, Jerusalem, Israel
Yan Q. Xiong: Geffen School of Medicine at UCLA, LABioMed at Harbor-UCLA Medical Center, Torrance, CA, USA

Introduction

Mupirocin was identified by computational methods as a good candidate for nano-liposomal delivery (1, 2). This computational approach tested the suitability of drugs for remote loading into liposomes and nano-liposomes. Remote liposomal loading is an approach by which preformed liposomes having an ion and/or pH gradient demonstrate a highly efficient and stable uptake of active pharmaceutical ingredients (APIs) (3, 4). Nano-liposomes remote loading may be the only valid solution to achieve enough drug per liposome to result in therapeutic efficacy in humans. Suitable candidates for remote loading are amphipathic weak acids or weak bases. These are defined by their logD at pH 7.0 in the range of –2.5 to 2.0. Amphipathic weak bases should have a pKa ≤11 and weak acids should have a pKa >3 (5). However, not all amphipathic weak acids or bases are suitable for this loading method. Computational screening identified only 2.3% of screened molecules as being capable of high and efficient remote loading into nano-liposomes (2). Mupirocin chemical structure is described by Figure 1. It is an amphipathic weak acid as defined by its pKa (4.78) and logD value at pH 7.0 (0.02) (6). In addition, it was highly scored by the computational models developed (2). Nano-liposomal formulation of mupirocin was developed based on this computational

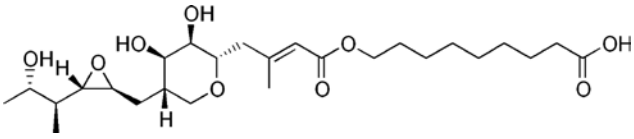

Figure 1: Mupirocin chemical structure.

approach (7, 8). This formulation, termed "Nano-mupirocin", is based on a PEGylated nano-liposomal formulation of mupirocin containing hydroxypropyl-β-cyclodextrin (HPCD) in its intra-liposomal aqueous phase. The HPCD in the liposomes improves the control of mupirocin release in the presence of serum. Figure 2 is a schematic illustration of mupirocin loading into calcium acetate liposomes with and without HPCD. Nano-mupirocin was found to be stable upon storage at 4°C for at least 1 year.

Mupirocin (pseudomonic acid A) is the major component of a family of structurally related antibiotics produced by strains of *Pseudomonas fluorescens* (9–11). The primary mode of action of mupirocin has been found to be inhibition of RNA and protein synthesis. The target in the bacterial cell is the isoleucine-binding site on the isoleucyl-transfer-RNA synthetase enzyme. By reversibly inhibiting formation of the enzyme complex, further incorporation of the amino acid is prevented, and cellular levels of the isoleucine charged transfer RNA are depleted. This causes cessation of RNA and protein synthesis in these bacteria. Mupirocin has low affinity for mammalian isoleucyl-transfer-RNA synthetase (12). Mupirocin's mode of action is unique and not shared by any other therapeutically available antibiotic, so that cross resistance with other antibiotics is not expected.

Mupirocin is active mainly against Gram-positive bacteria such as *Staphylococcus* and *Streptococcus*. The Gram-negative bacteria sensitive to mupirocin include *Haemophilus influenzae, Neisseria gonorrhoeae, Neisseria meningitides, Branhamella catarrhalis and Pasteurella multocida* (13). The Centers for Disease Control and Prevention (CDC) published the report "Antibiotic resistance threats in the United States, 2013" (14), which prioritized bacteria in this report into three categories: *urgent*, *serious*, and *concerning*. Mupirocin is active against bacteria in all three categories.

Mupirocin use is currently limited to topical administration due to its rapid degradation in vivo to its inactive metabolite (monic acid) and its high protein binding (9). The toxicity of mupirocin was studied after parenteral administration and it was found to be safe at therapeutically relevant doses (LD50 in mice and rats after IV administration was 1.6 and 1.3 g/kg, respectively) (13). Mupirocin was administered by intravenous infusion to human volunteers. The highest dose administered was 252 mg. The administered doses were well tolerated and there were no side effects (15).

We developed Nano-mupirocin to enable mupirocin parenteral use by encapsulation of mupirocin in long-circulating PEGylated nano-liposomes. Remote loading serves at least two functions: first, protecting mupirocin from degradation while circulating in the blood and second, enabling its passive targeting to the diseased tissue by taking advantage of the enhanced permeability and retention (EPR) effect in such tissues (7, 16). The EPR effect is the property by which macromolecules and nano-particlutes tend to preferentially accumulate at sites of increased vascular permeability. The EPR effect was

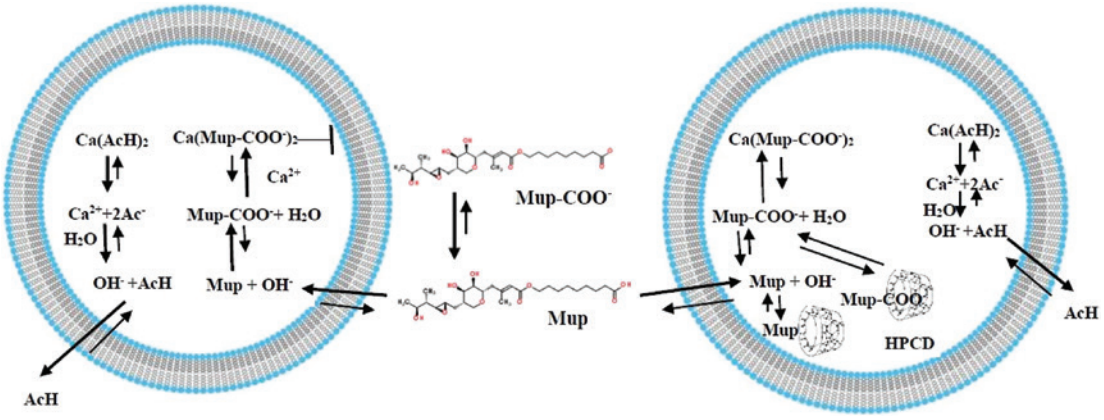

Figure 2: Remote loading of mupirocin into liposomes using a transmembrane calcium acetate gradient, (left scheme). Mupirocin in its un-ionized form influxes across the liposome membrane; it is then ionized inside the liposome and trapped by forming an insoluble salt with calcium. Concomitantly acetate is protonated to acetic acid and effluxes through the liposome membrane. For each acetate molecule that was effluxed, one molecule of mupirocin was influxed. This exchange process can continue until the liposome will lose all its acetate. However, in practice this exchange process is stopped much earlier as the retained trans-membrane calcium acetate gradient stabilizes the drug remote loading (31). The scheme on right shows loading of mupirocin into nano-liposomes exhibiting a tansmembrane gradient of calcium acetate which also contain HPCD (present in the figure in its toroid structure). HPCD ensures a controlled, slow mupirocin release in plasma (7).

taken advantage-of for the development of nano-drugs used to treat cancer and inflammation (17, 18). The EPR effect could also be used for antimicrobial delivery where it enables targeted antibiotic delivery (16). Encapsulating antibiotic drugs in liposomes may result in better antibacterial effects than the free drugs. This was demonstrated for amikacin and streptomycin encapsulated in liposomes. When injected to mice infected with *Mycobacterium avium*-intracellular complex (MAC) the liposomal encapsulated drugs showed higher therapeutic efficacy compared to the injections of the free drugs (19). Liposomal ciprofloxacin has been evaluated in a murine model of *Salmonella dublin* infection. Injection of liposomal ciprofloxacin was 10 times more effective in preventing mortality than injection of free drug (19). Arikace® (liposomal amikacin) for inhalation has currently completed successfully a phase III study with chronic *Pseudomonas aeruginosa* infections in cystic fibrosis patients (20). Other antibiotics encapsulated in liposomes and their in vivo activity may be found in the literature (21–24).

We present here our study of the in vivo effect of Nano-mupirocin in two clinically relevant animal models, mice in a *necrotizing fasciitis* model (25) in which the infection site is the skin and soft tissue, and rabbit *endocarditis* (26) in which the infection site is in the aortic valve of the heart. We found that Nano-mupirocin (given IV) is superior to the free drug in both animal models. In addition, Nano-mupirocin demonstrated a pharmacokinetic (PK) profile having much higher exposure (in terms of AUC) and much longer half-life than the free drug. This may explain the much better therapeutic efficacy of Nano-mupirocin. These results demonstrate for the first time that delivery of mupirocin as Nano-mupirocin enables its use as a parenteral therapeutically efficacious antibiotic. It has a unique mode of action, activity against resistant pathogens, and a good safety profile. In addition, Nano-mupirocin, due to the ability to benefit from the EPR effect, has the advantage of passively targeted delivery to the infected tissue. As shown by its PK profile, free mupirocin has very poor activity due to its rapid elimination and activity can be achieved only by reaching the target site through the EPR effect. Nano-mupirocin may show its activity mainly locally in target organs in which it will not be inactivated by metabolism and binding to proteins. It has the benefit of being administered parenterally, and thereby can affect internal organs, with low systemic exposure to the free drug that may cause toxicity. Topical routes of administration (pulmonary, intranasal, etc.) also show low systemic exposure with high concentration at the administration site but their effect is limited to the specific exposed organ.

The fact that Nano-mupirocin delivers sufficient amounts of active mupirocin to the infected tissue explains its superiority for the treatment of mice with *necrotizing fasciitis* and of rabbits with *endocarditis*. This opens the door to use Nano-mupirocin for the treatment of diseases that today represent a challenge such as deep infections with resistant bacteria. Nano-mupirocin having a unique mode of action as well as passive delivery to the infection site suggests a new mode of action (lack of cross resistance with other antibiotics) and benefit of passive targeting to the infected tissue.

Materials and methods

Materials

Mupirocin was a gift from Teva Pharmaceutical Industries Ltd. (Be'er Sheva, Israel) HPCD was a gift from Roquette Frères (Lestrem, France). The anion exchanger Dowex 1×8-200 and collagenase (type XI) were obtained from Sigma Aldrich (Saint Louis, MO, USA). Hydrogenated soy phosphatidylcholine (HSPC), 1,2-distearoyl-*sn*-glycero-3-phosphoethanolamine-N-[methoxy(polyethylene glycol)-2000] (mPEG DSPE) and cholesterol were obtained from Lipoid GmbH (Ludwigshafen, Germany). The solvents used for analysis were HPLC grade. All other chemicals were commercial products of reagent grade.

Methods

Preparation of Nano-mupirocin: PEGylated nano-liposomal formulation of mupirocin: Liposomes were prepared as described previously (7). Briefly, lipids in a mole ratio of 55:40:5 HSPC: cholesterol: mPEG DSPE were mechanically hydrated by stirring at 65°C with 200 mM calcium acetate pH 5.5 containing 15% (w/w) HPCD. The liposomal dispersion was downsized by stepwise extrusion by the Northern Lipids (Burnaby, BC, Canada) extruder using polycarbonate filter membranes. Liposomes were diafiltrated against a 10% sucrose solution using Millipore, Pellicon XL. Remote loading was performed by incubating at 65°C for 10 min a solution of the drug in 200 mM phosphate buffer, pH 6.3, with the liposome dispersion.

Mice necrotizing fasciitis model: The *necrotizing fasciitis* model was based on a published method (25). Female Balb/c mice, 3–4 weeks old (Envigo, Israel) ~10 g, were subcutaneously injected with approximately 1×10^8 CFU, M14 Group A streptococcus (GAS). GAS was cultured in Todd–Hewitt broth supplemented with 0.2% (w/v) yeast extract (THY) at 37°C.

The injection of the bacteria causes a wound in the skin, followed by a systemic disease characterized by difficulty in mobility, closed/partially closed eyes, rough hair, body weight loss and mortality. Mice were monitored for five days after bacterial challenge to evaluate disease severity and mortality. The minimum inhibitory concentration (MIC) of mupirocin to the GAS used was tested by the E test kit (BIOMERIEUX, MUPIROCIN MU 1024 US) and found to be <0.064 μg/mL.

PK study in mice: Free mupirocin (5 mg/mL solution in phosphate buffer 200 mM, pH 6.3) and Nano-mupirocin (5 mg/mL Nano-mupirocin containing 45 mg/mL lipids) were administered IV at a dose of 40 mg/kg to female Balb/c mice (Envigo, Israel) aged, 7–8 weeks. At the time points described below, mice (n=4 per time point) were humanely sacrificed with an overdose of intraperitoneal (IP) pentobarbital sodium. Terminal blood was collected in K3EDTA tubes and plasma was separated for the analysis. Time points for Nano-mupirocin were 1 min, 1 h, 4 h, 5.75 h and 24 h after drug administration. Time points for free mupirocin were 1 min, 5 min, 15 min, 30 min, 1 h and 4 h after drug administration.

A PK study in the mice with *necrotizing fasciitis* was additionally performed. In this study, free mupirocin or Nano-mupirocin at 40 mg/kg was administered 1 h after the bacterial challenge. At 1 h, 3 h and 24 h after drug administration, five mice of each group were sacrificed, and, in addition to collecting plasma as above, the wound and surrounding skin was excised.

The protocols of mice studies were approved by the Institutional Animal Care and Use Committee (IACUC) of the Hebrew University and Hadassah Medical Center for animal welfare.

PK parameters in plasma were calculated using WinNonlin 6.4 software (Pharsight Corp., A Certara company, NJ, USA).

Experimental *endocarditis* in rabbits caused by methicillin-resistant *Staphylococcus aureus* (MRSA): A well-characterized rabbit *endocarditis* model was used to evaluate the efficacy of Nano-mupirocin vs. free mupirocin, as previously described (27). At 72 h after aortic catheter placement, New Zealand white rabbits (2.2–2.5 kg) were infected by an MRSA strain, MW2 (USA400), using an ID_{95} dose (~10^5 CFU/animal) as we previously defined (27). At 24 h after induction of *endocarditis*, animals were equally randomized to the following groups (8 animals/group): (i) control (NaCl 0.9%, IV); (ii) free mupirocin at 25 mg/kg, IV, twice daily; or (iii) Nano-mupirocin at 25 mg/kg, IV, twice daily. Treatment lasted for 3 days. At 24 h after the last therapeutic dose, antibiotic-treated animals were sacrificed. Five control animals were euthanized at 24 h post-infection and three animals were not sacrifice at 24 h post-infection to determine the progress of infection. At sacrifice, cardiac vegetations, kidneys and spleens were removed, homogenized and quantitatively cultured. Target tissue counts were calculated from each therapy group, and expressed as mean $\log_{10}$ CFU/g tissue±SD.

The IACUC of the Los Angeles Biomedical Research Institute at Harbor-UCLA Medical Center approved this study protocol.

PK study in rabbits: PK blood samples were taken from two rabbits receiving Nano-mupirocin and one rabbit receiving free mupirocin. Time points for Nano-mupirocin PK samples were 5, 60, 120 and 240 min after the first dose administration. Time points for free mupirocin rabbit were 5, 15, 30 and 60 min after the first dose administration. Plasma was separated from the blood samples and processed as described below in mupirocin quantification in PK samples.

Analytical methods

Mupirocin quantification in the formulation: Drug concentrations were quantified using HPLC equipped with a UV detector (YL9100, YL Instruments, South Korea). The column used was a Luna C18 column, 5 µm, 4.6 mm×150 mm (Phenomenex, Torrance, CA, USA). The chromatographic conditions were based on a published USP method (28). Total (free plus liposomal) drug concentration was determined by HPLC assay of the liposomal dispersion diluted with methanol. Liposomal drug concentration was determined after removing the free drug by mixing the dispersion with Dowex 1×8–200 anion exchanger, which binds selectively the negatively charged free drug (29, 30).

Mupirocin quantification in PK samples: The chromatographic conditions used for the analysis of PK samples were identical to those used for the analysis of the formulation. Plasma samples were diluted with acetonitrile (five-fold dilution) followed by vortex and centrifugation. The diluted sample was analyzed by HPLC after additional dilution with water. In case of low drug concentration, samples were further evaporated to dryness and reconstituted to a 10-fold lower volume with methanol.

For the determination of drug biodistribution into the skin wounds in the mice *necrotizing fasciitis* model, wound samples were weighed and incubated with 1 mL of collagenase solution (0.75 mg/mL solution containing also calcium chloride, 0.3 mg/mL) by shaking (200 rpm), at 37°C. After overnight incubation, samples were diluted five-fold with acetonitrile, vortexed, and the upper phase was evaporated to dryness and reconstituted with methanol prior to HPLC analysis.

Sample preparation process of both plasma and wound samples was verified by spiking of control samples with known amounts of mupirocin, resulting in >90% recovery.

Results and discussion

The Nano-mupirocin formulation was designed, as previously described, based on a computational approach to identify molecules suitable for remote liposomal loading (2, 7). The remote loading of mupirocin (which is a weak amphipathic acid) into PEGylated nano-liposomes is driven by a transmembrane calcium acetate gradient (31, 32). The Nano-mupirocin formulation obtained was stable upon storage at 4°C (for at least 1 year, study ongoing). However, in serum at 37°C, drug release was fast (82% release within 1 h) (7). The presence of HPCD in the intra-liposomal volume slowed down this fast release (7). The product of PEGylated nano-liposomes containing HPCD and remotely loaded with mupirocin is termed "Nano-mupirocin". The intra-liposomal concentration of mupirocin was calculated from the liposomal trapped aqueous volume, which was determined from the liposome trapped calcium. Intra-liposome aqueous phase mupirocin concentration was found to be ~200 mM (~100 mg/mL), which is much higher than mupirocin's solubility (mupirocin maximal solubility in 15% HPCD in phosphate buffer pH 6.3 is 82 mM). This results in an intra-liposomal HPCD to mupirocin mole ratio of ~1 to 2 (200 mM mupirocin to 109 mM HPCD). A schematic illustration of mupirocin loading into calcium acetate liposomes with and without HPCD is given in Figure 2. Nano-mupirocin's particle size is ~85 nm (z average) and its polydispersity index of 0.09

indicates a narrow unimodal size distribution. The stability of the formulation upon storage at 4°C was followed for 1 year. Nano-mupirocin was found to be stable in terms of drug leakage, drug concentration and particle size. This stability study is still ongoing.

In this study we describe the first in vivo evaluations of Nano-mupirocin.

Efficacy of Nano-mupirocin and free mupirocin in a mice *necrotizing fasciitis* model

The mice *necrotizing fasciitis* model was used for a proof of concept study to test whether Nano-mupirocin can demonstrate efficacy when administered intravenously. In this model, mice were challenged with GAS subcutaneously, resulting in the development of a wound at the injection site and systemic disease 24–48 h after the bacterial challenge. In addition to wound development, infected mice show rough hair, difficulty in mobility, closed/partially closed eyes and reduction in body weight.

In the first study, mice received either one prophylactic IV dose of 50 mg/kg/day Nano-mupirocin 3 h before the bacterial challenge or three IV injections of free mupirocin (50 mg/kg each, total of 150 mg/kg/day: 1, 3 h before the bacterial challenge followed by a second and third, 3 and 24 h after the bacterial challenge). The results describing mortality and disease status 48 h after the bacterial challenge are presented in Figure 3A. Two mice out of six died in the untreated group 48 h after the bacterial challenge. Other mice in this group showed disease signs of rough hair and wound development. In the free mupirocin group, mice had rough hair and large wounds, while in the Nano-mupirocin group all mice showed no signs of disease. In addition, 48 h after the bacterial challenge mice in the untreated and free-mupirocin group lost on average 6.4% and 1.9% of their body weight, respectively, while in the Nano-mupirocin group, animals gained an average of 7.5% of their body weight (mice were weighed as a group and not individually).

Figure 4 is a photograph comparing a typical Nano-mupirocin-treated mouse with an untreated one. The untreated mouse has rough hair with a large wound, while the Nano-mupirocin-treated mouse has smooth, regular hair and no wound (hair was removed prior to injection of bacteria).

The second study tested the efficacy of three prophylactic doses of Nano-mupirocin vs. no treatment. Figure 3B shows that five out of six mice died in the control group, with no mortality in either of the Nano-mupirocin groups. In the 15 mg/kg group, one mouse showed rough hair and

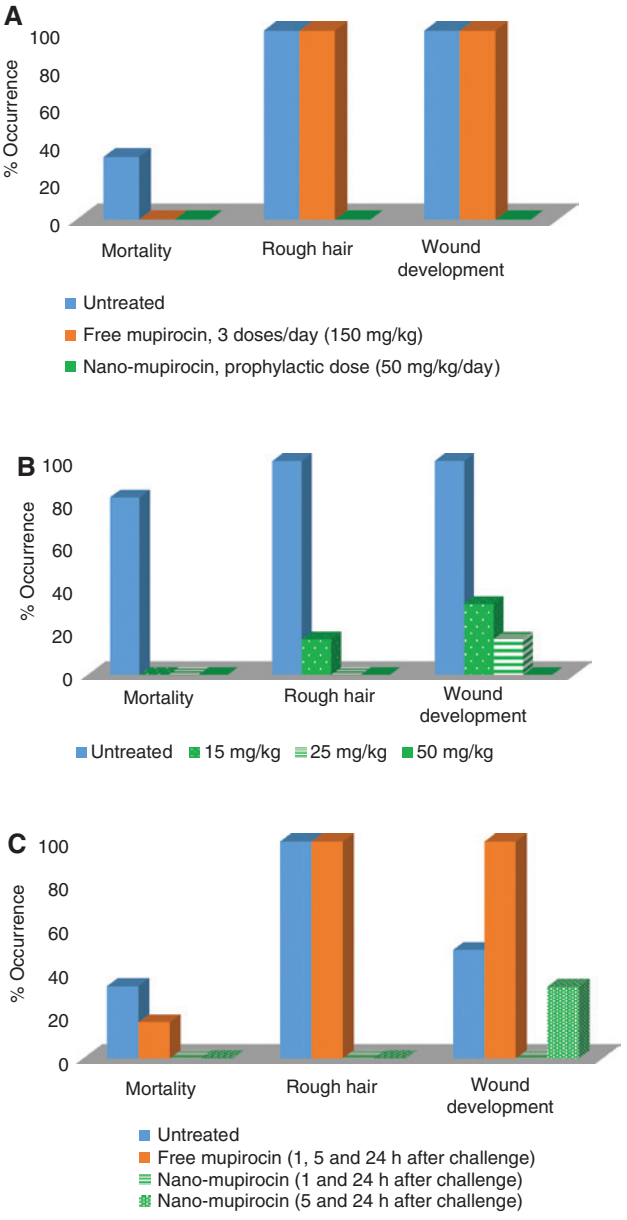

Figure 3: Mortality during the study and disease parameters (rough hair and wound development) 48 h after the bacterial challenge. (A) A study to compare one prophylactic dose of Nano-mupirocin (50 mg/kg) vs. free mupirocin administered prophylactically and 3 and 24 h after the bacterial challenge. (B) A prophylactic dose response study. (C) Nano-mupirocin administration after the bacterial challenge vs. free mupirocin administration.

two developed wounds. Except for that, mice in the Nano-mupirocin groups did not show signs of the disease. Mice in the untreated group lost an average of 7.4% of their body weight 48 h after the bacterial challenge compared to body weight gain of 3.8%, 9.2% and 8.9% in those treated with 15 mg/kg, 25 mg/kg and 50 mg/kg, respectively.

An additional study tested the efficacy of Nano-mupirocin at 50 mg/kg intraperitoneal (IP) dose given

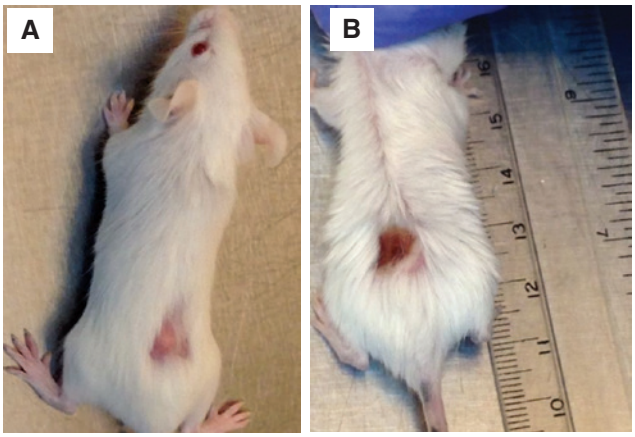

Figure 4: Appearance of a typical Nano-mupirocin-treated mouse (A) vs. an untreated one (B) 24 h after bacterial challenge. (Hair was removed prior to injection of bacteria.)

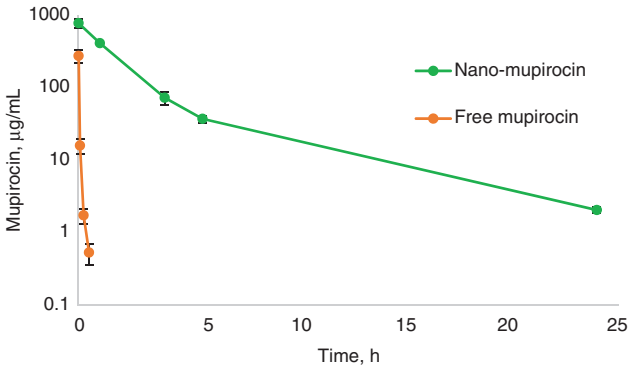

Figure 5: Plasma profile of mupirocin after IV administration of 40 mg/kg free vs. Nano-mupirocin.

1 h or 5 h after the bacterial challenge vs. free mupirocin administration (see Figure 3C). Two animals died in the control and one animal died in the free mupirocin groups. Other animals in the free mupirocin group showed rough hair and wound development. Nano-mupirocin-treated mice did not show disease symptoms, with the exception of two animals treated 5 h after the bacterial challenge that showed a small/medium wound. This study demonstrated that Nano-mupirocin was effective as treatment (after the challenge) and not only as prophylaxis.

In general, no mortality occurred in Nano-mupirocin-treated mice in the three studies described, compared to 33–83% mortality in the control groups of the three studies.

Mice pharmacokinetic profile of Nano-mupirocin vs. free mupirocin

The PK profiles of Nano-mupirocin and free mupirocin were determined in healthy mice following IV administration of 40 mg/kg dose. Figure 5 presents the PK profiles obtained. Nano-mupirocin resulted in enormously higher mupirocin plasma levels. After administration of Nano-mupirocin, detectable levels of mupirocin were observed until the last experimental time point tested (24 h). Administration of free mupirocin resulted in a much faster decrease in mupirocin levels, and 15 min after administration there were only very low levels (average of 1.7 µg/mL). Table 1 summarizes the PK parameters obtained. Note that due to the rapid elimination of free mupirocin from plasma, it is assumed that most of the mupirocin in plasma after administration of Nano-mupirocin is encapsulated in liposomes. The AUC of mupirocin after administration of free mupirocin was only 1% of the AUC obtained after administration of Nano-mupirocin. The half-life of mupirocin after administration of the free drug was calculated to be 5 min, while by administration of Nano-mupirocin the half-life was substantially increased to 4.4 h. (Note that the half-life obtained for Nano-mupirocin is dependent on the last two time points. This value would probably have been increased if additional time points were measured.) The MIC of mupirocin to GAS used for the in vivo study was determined by E test to be <0.064 µg/mL. Nano-mupirocin AUC/MIC value is therefore 1.65E+06 and Cmax/MIC value is 1.29E+04.

The levels of mupirocin following IV administration of Nano-mupirocin and free mupirocin were also evaluated at three time points in mice in a *necrotizing fasciitis* model (efficacy of Nano-mupirocin and free mupirocin in a mice *necrotizing fasciitis* model). One hour after the bacterial challenge, either Nano-mupirocin or free mupirocin was

Table 1: Pharmacokinetic parameters of Nano-mupirocin vs. free mupirocin.

	$t_{1/2}$, min	Cmax, µg/mL	C_0, µg/mL	AUCz, min*µg/mL	AUC∞, min*µg/mL	CL, mL/min/kg
Nano-mupirocin	262	771	780	105,771	106,477	0.38
Free mupirocin	5.28	273	557	1096	1100	36.4

Cmax, Maximum plasma concentration; C_0, extrapolated concentration at t=0; AUCz, the area under the curve from time of dosing to the last time point calculated by the logarithmic trapezoidal method; AUC∞, AUC extrapolated to infinity. Calculated from the following equation: AUC∞=AUCz+Cz/λ where Cz is the concentration at last time point predicted by the linear regression and λ is the terminal slope; CL, clearance was calculated from the following equation: CL=Dose /AUC∞.

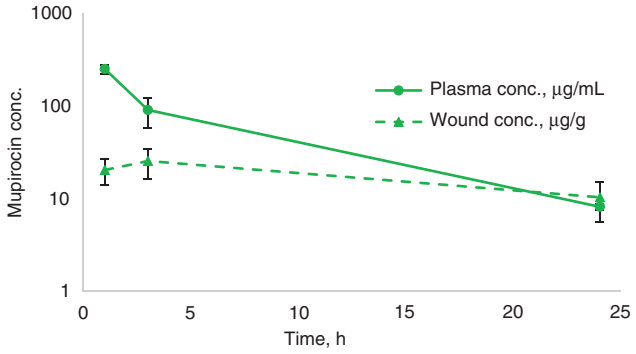

Figure 6: Mupirocin plasma and wound concentrations after administration of Nano-mupirocin to diseased mice.

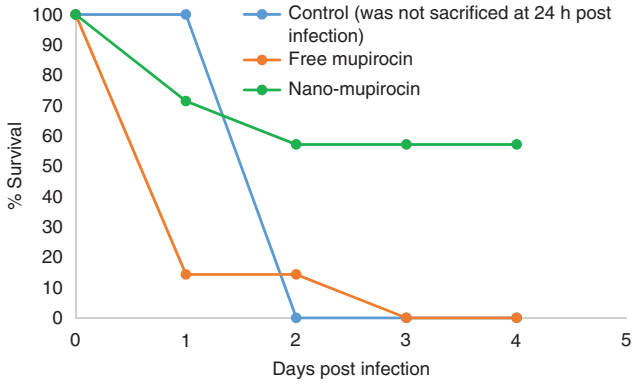

Figure 7: Percent survival of rabbits in *endocarditis* study across the treatment groups.

administered to diseased mice, and plasma and wounds were collected at 1, 3 and 24 h after drug administration. At the tested time points, no mupirocin was found in the plasma and wounds of mice receiving free mupirocin. Plasma and wounds concentrations at the three tested time points after administration of Nano-mupirocin are presented in Figure 6. Plasma levels following administration of Nano-mupirocin to diseased mice were very similar to those obtained for healthy mice, with the exception of the last time point (24 h), which for sick mice averaged 8.2 µg/mL vs. 2.0 µg/mL for healthy mice. Mupirocin concentrations in the wounds following administration of Nano-mupirocin were 20 and 25 µg/g at 1 and 3 h, respectively, and 10 µg/g at 24 h. All these concentrations are much higher than the MIC of mupirocin against GAS (<0.064 µg/mL).

Experimental *endocarditis* in rabbits caused by methicillin-resistant *Staphylococcus aureus*

Nano-mupirocin-treated animals had significantly higher survival as compared to free-mupirocin treatment group and the control group which was not sacrificed at 24 h post-infection (Figure 7; 57% survival for Nano-mupirocin vs. 0% survival for free mupirocin and control). In addition, Nano-mupirocin had significantly better efficacy in decreasing MRSA densities within all relevant target tissues of animals infected with MRSA strain, MW2 (USA400), in this model as compared to the control group that was not sacrificed at 24 h post-infection (Table 2).

The PK profiles of Nano-mupirocin and free mupirocin in rabbits are shown in Figure 8. The PK profiles were very similar to those found in mice showing rapid elimination of the free drug vs. high mupirocin levels after administration of Nano-mupirocin over the time tested.

Conclusions

Mupirocin is an antibiotic having special advantages: it has a unique mode of action not shared by any other therapeutically available antibiotic; it is considered to be safe at therapeutically relevant doses and it is active against resistant bacteria including *Neisseria gonorrhoeae*, MRSA and *Streptococcus pneumoniae*, which are classified by the CDC as urgent and serious threats to public health. However, due to its rapid metabolism and high protein binding, the administration of mupirocin is restricted to topical administration. Our computational approach identified mupirocin as a good

Table 2: MRSA densities in target tissues and percent survival after free- or Nano-mupirocin treatment in rabbit *endocarditis* model.

Group	Survival	Mean $\log_{10}$ CFU/g tissue±SD		
		Vegetation	Kidney	Spleen
Control (24 h post-infection)	5/5	8.12±0.41	6.21±0.62	6.58±0.57
Control (was not sacrificed at 24 h post-infection)	0/3[a]	8.89±0.23	8.21±0.35	7.32±0.45
Free-mupirocin (25 mg/kg, IV, bid×3 d)	0/7	8.23±0.68	7.31±0.64	6.35±0.63
Nano-mupirocin (25 mg/kg, IV, bid×3 d)	4/7	8.04±0.50[b]	6.93±0.30[c]	6.36±0.78[d]

[a]All animals were dead at 48 h post-infection. [b]p=0.006, MRSA densities in vegetation in Nano-mupirocin vs. control that was not sacrificed at 24 h post-infection. [c]p=0.009, MRSA densities in kidney in Nano-mupirocin vs. control that was not sacrificed at 24 h post-infection. [d]p=0.047, MRSA densities in spleen in Nano-mupirocin vs. control that was not sacrificed at 24 h post-infection.

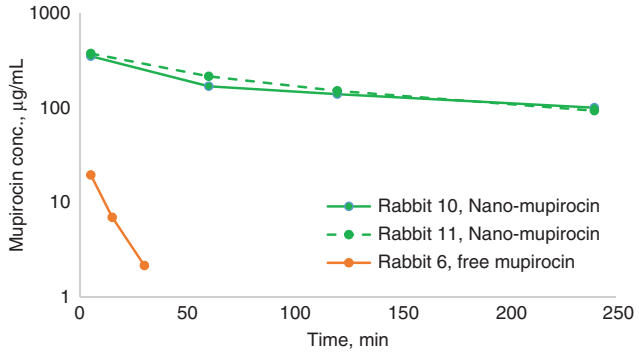

Figure 8: Mupirocin plasma concentrations after IV administration of 25 mg/kg Nano-mupirocin vs. free mupirocin.

candidate for remote liposomal loading, which led to the development of Nano-mupirocin, a PEGylated nano-liposomal formulation of mupirocin. This formulation showed stability upon storage at 4°C. Nano-mupirocin showed efficacy after injection in two animal models: mice *necrotizing fasciitis* and rabbit *endocarditis* models.

Nano-mupirocin efficacy in a mice *necrotizing fasciitis* model was shown when tested prophylactically at doses of 15, 25 and 50 mg/kg and when administered 5 h after the bacterial challenge.

In the rabbit *endocarditis* model, animals dosed with 25 mg/kg Nano-mupirocin twice daily showed 57% survival vs. no survival in the free mupirocin at the same dose regimen and untreated control groups.

The pharmacokinetics of Nano-mupirocin was tested in healthy and diseased mice. Administration of free mupirocin resulted in rapid decrease in mupirocin levels, and 15 min after administration only very low levels were quantified. Nano-mupirocin administration resulted in higher mupirocin plasma levels, which lasted until the last time point tested (24 h). The ratio of mupirocin AUC after administration of Nano-mupirocin to that of free mupirocin was 97:1. The high mupirocin concentrations obtained after administration of Nano-mupirocin are most probably from liposomal mupirocin and do not represent free mupirocin, as the free mupirocin is rapidly degraded. The PK profile of Nano-mupirocin may explain the efficacy of Nano-mupirocin; its long circulation time results in distribution of enough drug to the target site by the EPR effect. This was also shown by quantifying mupirocin concentrations in the wounds of diseased mice. The concentrations of mupirocin after injection of Nano-mupirocin in the wounds were 10–25 µg/mL at the time points tested vs. no quantifiable levels found in the wounds of animals treated with free mupirocin.

Similar PK profiles were shown in rabbits in the *endocarditis* model. As shown for the mice, following free mupirocin injection, mupirocin was rapidly eliminated, while rabbits treated with Nano-mupirocin showed high and prolonged mupirocin levels.

Nano-mupirocin is a passively targeted antibacterial formulation enabling for the first time the therapeutic activity of mupirocin by injection. The ability to use mupirocin parenterally results in a new parenteral antibiotic with a unique mode of action that may be useful for the treatment of resistant bacteria considered as threats to public health.

Acknowledgments: This study was supported by Kamin grant of The Chief Scientist at the Israeli Ministry of Economy and by the Barenholz Fund at the Hebrew University of Jerusalem. This fund originated from royalties Hebrew University received from Yechezkel Barenholz's commercialized projects. Part of this money is used to support the research activities of the Barenholz Lab. We authors would like to acknowledge Dr. Mary Dan-Goor for her help with the mice study. Mr. Sioma Nudelman and Mrs. Olga Gutman for their help in the preparation of Nano-mupirocin and Mr. Sigmund Geller for editing this paper.

Conflict of interest statement: Y. Barenholz, A. Goldblum and A. Cern are co-inventors on a patent application owned by Yissum, the TTO of the Hebrew University of Jerusalem, that was not yet commercialized.

References

1. Cern A, Golbraikh A, Sedykh A, Tropsha A, Barenholz Y, Goldblum A. Quantitative structure – property relationship modeling of remote liposome loading of drugs. J Control Release 2012;160:147–57.
2. Cern A, Barenholz Y, Tropsha A, Goldblum A. Computer-aided design of liposomal drugs: in silico prediction and experimental validation of drug candidates for liposomal remote loading. J Control Release 2014;173:125–31.
3. Barenholz Y. Liposome application: problems and prospects. Curr Opin Colloid Interface Sci 2001;6:66–77.
4. Barenholz Y. Relevancy of drug loading to liposomal formulation therapeutic efficacy. J Liposome Res 2003;13:1–8.
5. Zucker D, Marcus D, Barenholz Y, Goldblum A. Liposome drugs' loading efficiency: a working model based on loading conditions and drug's physicochemical properties. J Control Release 2009;139:73–80.
6. Advanced Chemistry Development Software V11.02.
7. Cern A, Nativ-Roth E, Goldblum A, Barenholz Y. Effect of solubilizing agents on mupirocin loading into and release from PEGylated nanoliposomes. J Pharm Sci 2014;103:2131–8.
8. Barenholz Y, Goldblum A, Cern A. Liposomal mupirocin. WO 2015/155773 A1, 2015.
9. Pappa K. The clinical development of mupirocin. J Am Acad Dermatol 1990;22:873–9.

10. Fuller A, Mellows G, Wollford M, Banks G, Barrow K, Chain E. Pseudomonic acid: an antibiotic produced by Pseudomonas fluorescens. Nature 1971;234:416–7.
11. Sutherland R, Boon RJ, Griffin KE, Masters PJ, Slocombe B, White AR. Antibacterial activity of mupirocin (pseudomonic acid), a new antibiotic for topical use. Antimicrob Agents Chemother 1985;27:495–8.
12. Hughes J, Mellows G. Interaction of pseudomonic acid A with Escherichia coli B isoleucyl-tRNA synthetase. Biochem J 1980;191:209–19.
13. GlaxoSmithKline Inc. Product monograph Bactroban.
14. U.S. Department of Health and Human Services Centers for Disease Control and Prevention. Antibiotic resistance threats in the United States, 2013. 2013.
15. Baines P, Jackson D, Mellows G, Swaisland A, Tasker T. Mupirocin: its chemistry and metabolism. In: Wilkinson D, Price J, editors. Mupirocin a novel topical antibiotic. Royal Society of Medicin, London (Distributed by Oxford University Press). International Congress and Symposium Series 80, 1984:13–22.
16. Azzopardi EA, Ferguson EL, Thomas DW. The enhanced permeability retention effect: a new paradigm for drug targeting in infection. J Antimicrob Chemother 2013;68:257–74.
17. Barenholz Y. Doxil® – The first FDA-approved nano-drug: lessons learned. J Control Release 2012;160:117–34.
18. Avnir Y, Ulmansky R, Wasserman V, Even-Chen S, Broyer M, Barenholz Y, et al. Amphipathic weak acid glucocorticoid prodrugs remote-loaded into sterically stabilized nanoliposomes evaluated in arthritic rats and in a Beagle dog: a novel approach to treating autoimmune arthritis. Arthritis Rheum 2008;58:119–29.
19. Salem II, Flasher DL, Düzgüneş N. Liposome-encapsulated antibiotics. Methods Enzymol 2005;391:261–91.
20. http://clinicaltrials.gov. Study to Evaluate Arikace™ in CF Patients With Chronic Pseudomonas Aeruginosa Infections.
21. Schiffelers RM, Storm G, Ten Kate MT, Stearne-Cullen LE, den Hollander JG, Verbrugh HA, et al. In vivo synergistic interaction of liposome-coencapsulated gentamicin and ceftazidime. J Pharmacol Exp Ther 2001;298:369–75.
22. Labana S, Pandey R, Sharma S, Khuller GK. Chemotherapeutic activity against murine tuberculosis of once weekly administered drugs (isoniazid and rifampicin) encapsulated in liposomes. Int J Antimicrob Agents 2002;20:2000–3.
23. Kadry AA, Al-Suwayeh SA, Abd-Allah ARA, Bayomi MA. Treatment of experimental osteomyelitis by liposomal antibiotics. J Antimicrob Chemother 2004;54:1103–8.
24. Wang D, Kong L, Wang J, He X, Li X, Xiao Y. Polymyxin E sulfate-loaded liposome for intravenous use: preparation, lyophilization, and toxicity assessment in vivo. PDA J Pharm Sci Technol 2009;63:159–67.
25. Hidalgo-Grass C, Dan-goor M, Maly A, Eran Y, Kwinn LA, Nizet V, et al. Effect of a bacterial pheromone peptide on host chemokine degradation in group A streptococcal necrotising soft-tissue infections. Mech Dis 2004;363:696–703.
26. Xiong YQ, Kupferwasser LI, Zack PM, Bayer AS. Comparative efficacies of liposomal amikacin (MiKasome) plus oxacillin versus conventional amikacin plus oxacillin in experimental endocarditis induced by Staphylococcus aureus: microbiological and echocardiographic analyses. Antimicrob Agents Chemother 1999;43:1737–42.
27. Abdelhady W, Bayer AS, Seidl K, Moormeier DE, Bayles KW, Cheung A, et al. Impact of vancomycin on sarA-mediated biofilm formation: role in persistent endovascular infections due to methicillin-resistant staphylococcus aureus. J Infect Dis 2014;209:1231–40.
28. USP 35. Mupirocin official monograph.
29. Druckmann S, Gabizon A, Barenholz Y. Separation of liposome-associated doxorubicin from non-liposome-associated doxorubicin in human plasma: implications for pharmacokinetic studies. Biochim Biophys Acta 1989;980:381–4.
30. Amselem S, Gabizon A, Barenholz Y. Optimization and upscaling of doxorubicin-containing liposomes for clinical use. J Pharm Sci 1990;79:1045–52.
31. Avnir Y, Turjeman K, Tulchinsky D, Sigal A, Kizelsztein P, Tzemach D, et al. Fabrication principles and their contribution to the superior in vivo therapeutic efficacy of nano-liposomes remote loaded with glucocorticoids. PLoS One 2011;6:e25721.
32. Clerc S, Barenholz Y. Loading of amphipathic weak acids into liposomes in response to transmembrane calcium acetate gradients. Biochim Biophys Acta 1995;1240:257–65.

Bionotes

Ahuva Cern
Laboratory of Membrane and Liposome Research, Department of Biochemistry, IMRIC, The Hebrew University – Hadassah Medical School, Jerusalem, Israel; and Molecular Modeling and Drug Design Laboratory, The Institute for Drug Research, The Hebrew University of Jerusalem, Israel

Ahuva Cern is a researcher at the Laboratory of Membrane and Liposome Research at the Hebrew University of Jerusalem. She is a pharmacist (Hebrew University) with MSc degree in Biomedical Engineering (Ben-Gurion University). Her PhD thesis was focused on computational models of liposome-based drugs. Her research interests are in the field of formulation development, drug delivery systems and their role in improving drug performance. Prior to this position, Ahuva was the director of the formulation development lab at Nextar Chempharma Solutions, where she managed many formulation development projects for pharma and biotech companies.

Ayelet Michael-Gayego
Microbial Molecular Diagnostics Laboratory, Department of Clinical Microbiology and Infectious Diseases, Hadassah Hebrew University Medical Center, Jerusalem, Israel

Ayelet Michael-Gayego is responsible for the microbial molecular diagnostic laboratory at the Department of Clinical Microbiology and Infectious Diseases, Hadassah University Medical Center, Jerusalem. Her research interests focused on gene therapy using viral vectors and virulence mechanisms of group A and group G streptococci.

During her PhD studies, she worked on characterization of the necrotizing fasciitis model in mice. She received the Dean's award of excellence.

Yaelle Bavli
Laboratory of Membrane and Liposome Research, Department of Biochemistry, IMRIC, The Hebrew University – Hadassah Medical School, Jerusalem, Israel

Yaelle Bavli is a PhD student at the Laboratory of Membrane and Liposome Research at the Hebrew University of Jerusalem. She has an MSc in Pharmacology with a specialization in pre-clinical models from the Louis Pasteur University of Strasbourg, France. Her PhD research interests include procedures to evaluate in animal models the adverse effects of local and systemic injection of nano-liposomal drugs (including complement activation, CARPA, macrophage depletion and accelerated blood clearance).

Erez Koren
Laboratory of Membrane and Liposome Research, Department of Biochemistry, IMRIC, The Hebrew University – Hadassah Medical School, Jerusalem, Israel

Erez Koren is currently employed at Teva Pharmaceuticals in Israel. As a team leader in the Innovative R&D discovery and product development group, the main focus of his team is oral dosage forms and novel injectable formulations and technologies. Prior to this position, he was working for 3 years at Lipocure Ltd as a project manager where he was focused on developing a number of highly-potent therapeutics utilizing proprietary liposome-based nano-drugs with novel drug-loading-capabilities and drug-release mechanisms. Erez is a graduate of the School of Pharmacy, The Hebrew University of Jerusalem, Israel, with a PhD in Pharmaceutical Sciences. He also completed a post-doctoral fellowship in pharmaceutical sciences with special focus on liposomal and micellar drug delivery at Prof. Vladimir Torchilin's lab, Northeastern University, Boston, MA.

Amiram Goldblum
Molecular Modeling and Drug Design Laboratory, The Institute for Drug Research, The Hebrew University of Jerusalem, Israel

Amiram Goldblum is Head of Molecular Modeling and Drug Design unit at the Institute for Drug Research of the Hebrew University of Jerusalem. Studied Chemistry and Physics and continued Post-doctoral Studies on Quantum Biochemistry (Paris), Quantitative Structure-Activity Relations and Quantum Mechanics of reaction pathways (California). Developed a prize winning computer algorithm that has been applied to problems in structural biology, protein-ligand and protein-protein interactions, molecular design of small molecules, of peptides and of proteins, and more recently, to cheminformatics and informatics. Amiram Goldblum is a board Member of The Lisa Meitner Minerva Center for Computational Quantum Chemistry, Served as the Chairperson of the 1996 conference of The World Organization of Theoretically Oriented Chemists.

Allon E. Moses
Department of Clinical Microbiology and Infectious Diseases, Hadassah Hebrew University Medical Center, Jerusalem, Israel

Allon E. Moses Allon Moses is a physician-scientist. He studied medicine at the Beer Sheva University Medical School and specialized in Internal Medicine at the Hadassah Hebrew University Medical Center and in Infectious Diseases at the Harvard Combined Infectious Diseases Program. He is currently Chairman of the Department of Clinical Microbiology and Infectious Diseases at the Hadassah Hebrew University Medical Center in Jerusalem. He was previous Chairman of the Israel Society of infectious diseases. His main interests are pathogenesis of infectious diseases at the molecular level especially group A and G hemolytic streptococci. He is also intensely involved in infection control and prevention of bacterial resistance and nosocomial infections.

Yan Q. Xiong
Geffen School of Medicine at UCLA, LABioMed at Harbor-UCLA Medical Center, Torrance, CA, USA

Yan Q. Xiong is a Professor of Research at the David Geffen School of Medicine at UCLA, a senior investigator at Harbor-UCLA Medical Center and a key faculty member in the Division of Infectious Diseases at LABioMed at Harbor-UCLA. After her medical degree from Tongji Medical University, China, she earned a PhD from the Universite of Nantes, France, and then she completed a post-doctoral fellowship in infectious diseases at Harbor-UCLA. Her research program focuses on the role of *Staphylococcus aureus* virulence factors (global regulons and structural genes) that contribute to the ability of this pathogen to cause human disease and resist antibiotics. Her area of intensive interest includes bacterial pathogenesis and antibiotic resistance in endovascular infections. Her long-term goal is to discover novel antimicrobial strategies for the prevention and therapy of serious infections caused by virulent microbes, including MRSA. She has published more than 100 research articles in peer-reviewed journals, and has served as the Principal Investigator on NIH and American Heart Association grant awards.

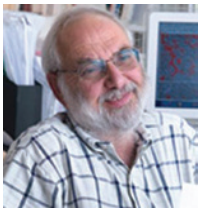

Yechezkel Barenholz
Laboratory of Membrane and Liposome Research, Department of Biochemistry, IMRIC, The Hebrew University – Hadassah Medical School, Jerusalem, Israel
Phone: +972 2 6757615,
Fax: +972 2 6757499,
chezyb@ekmd.huji.ac.il

Yechezkel Barenholz (Daniel G. Miller Professor in Cancer Research), the head of Liposome and Membrane Research Lab has been on the faculty of Hebrew University Jerusalem Israel since 1968 and has been a Professor there since 1981, a visiting Professor at the University of Virginia School of Medicine, Charlottesville VA, USA (1973 to 2005); a Donder's Chair Professor at The Faculty of Pharmacy, University of Utrecht, The Netherlands on 1992; the University Kyoto University (Kyoto, Japan, 1998), La Sapeinza University (Roma, Italy, 2006) Jaiotung University (Shanghai, China, 2006), Kings College (London, UK, 2006), the Technical University Of Denmark (Copenhagen 2010). His current research focuses on the development of drugs based on drug delivery systems (DDS) best exemplified by the anticancer DOXILTM the first nano liposomal and the first FDA approved (1995) nano-drug used world-wide. Professor Barenholz is an author of more than 380 scientific publications having altogether more than 10,000 citations. He is a co-inventor of more than 30 approved patent families. He was an executive editor of *Progress in Lipid Research*, an editor of four Special Issues, and is on the editorial board of five scientific journals. Professor Barenholz is a founder of Mobeius Medical LTD, Lipocure LTD, and Doxocure LTD all are in advanced stage of development of liposomal drugs based on Professor Barenholz inventions and knowhow. Professor Barenholz was awarded: the Donder's Chair, the Kaye award twice (1995 and 1997), the Alec D. Bangham (the Liposome research "father") award (1998), the Teva Founders Prize (2001), an Honorary Doctor degree from the Technical University of Denmark (DTU) in 2012, and the international Controlled Release Society's (CRS) CRS Founders Award for 2012. In 2003 Professor Barenholz founded (from DOXIL royalties) the "Barenholz Prize" to encourage excellence and innovation in applied science of PhD students in Israel.